Bacillus Calmette-Guerin (BCG) induces superior anti-tumour responses by Vδ2^{+} T-cells compared to the aminobisphosphonate drug Zoledronic acid

J Fenn* [1,2], L A Ridgley* [1], A White[3], C Sarfas[3], M Dennis[3], A Dalgleish[1], R Reljic[1], S Sharpe[3], M Bodman-Smith[1]

* These authors contributed equally to this manuscript

[1] St George's University of London, Institute for Infection and Immunity, Cranmer Terrace, London, SW17 0RE

[2] Imperial College London Faculty of Medicine, National Heart and Lung Institute, St. Mary's hospital, Praed Street, London, UK W2 1NY

[3] UK Health Security Agency, Porton Down, Salisbury, SP4 0JG

Abbreviations:

- BCG - Bacillus Calmette–Guérin
- BTN3A1 - Butyrophilin 3A1
- CFU – colony forming unit
- DAPI - 4', 6-diamidino-2-phenylindole
- DC – Dendritic cell
- DMSO - Dimethyl sulfoxide
- ECACC- European Collection of Authenticated Cell Cultures
- EDTA - Ethylenediaminetetraacetic acid
- FACS- fluorescence-activated cell sorting
- FBS - Foetal Bovine Serum
- FPPS - Farnesyl pyrophosphate synthase
- GFP – Green fluorescent protein
- HKBCG – Heat killed Bacillus Calmette–Guérin
- HMBPP - (E)-4-hydroxy-3-methyl-but-2-enyl pyrophosphate
- IPP - Isopentenyl pyrophosphate
- MACS – magnetic activated cell sorting
- mGLP - 6-O-methylglucose-containing lipopolysaccharides
- MOI – multiplicity of infection
- NHSBT - NHS Blood and Transplant
- NK – Natural killer
- pAgs - Phosphate antigens
- PBMC – peripheral blood mononucrlear cell

- PMA - Phorbol 12-myristate 13-acetate
- PPD – purified protein derivative
- RPMI - Roswell Park Memorial Institute
- tSNE - t-distributed stochastic neighbor embedding
- ZA – Zoledronic acid

Corresponding author: Joe Fenn

Imperial College London Faculty of Medicine

National Heart and Lung Institute

St. Mary's hospital

Praed Street

London

UK W2 1NY

jfenn@ic.ac.uk

020 3312 6666

Abstract

Vδ2$^+$ T-cells can recognise malignantly transformed cells as well as those infected with mycobacteria. This cross-reactivity supports the idea of using mycobacteria to manipulate Vδ2$^+$ T-cells in cancer immunotherapy. To date, therapeutic interventions using Vδ2$^+$ T-cells in cancer have involved expanding these cells *in* or *ex vivo* using zoledronic acid (ZA). Here, we show that the mycobacterium Bacillus Calmette–Guérin (BCG) also causes Vδ2$^+$ T-cell expansion *in vitro* and that resulting Vδ2$^+$ cell populations are cytotoxic towards tumour cell lines. We show that both ZA and BCG-expanded Vδ2+ cells effectively killed both Daudi and THP-1 cells. THP-1 cell killing by both ZA and BCG-expanded Vδ2+ cells was enhanced by treatment of targets cells with ZA. Although no difference in cytotoxic activity between ZA- and BCG-expanded Vδ2+ cells was observed, BCG-expanded cells degranulated more and produced a more diverse range of cytokines upon tumour cell recognition compared to ZA-expanded cells. ZA-expanded Vδ2+ cells were shown to upregulate exhaustion marker CD57 to a greater extent than BCG-expanded Vδ2+ cells. Furthermore, ZA expansion was associated with upregulation of inhibitory markers PD-1 and TIM3 in a dose-dependent manner whereas PD-1 expression was not increased following expansion using BCG. Intradermal BCG vaccination of rhesus macaques caused *in vivo* expansion of Vδ2$^+$ cells. In combination with the aforementioned *in vitro* data, this finding suggests that BCG treatment could induce expansion of Vδ2$^+$ T-cells with enhanced anti-tumour potential compared to ZA treatment and that either ZA or BCG could be used intratumourally as a means to potentiate stronger anti-tumour Vδ2$^+$ T-cell responses.

Key words: γδ T cell, cancer, mycobacteria, BCG

Graphical abstract

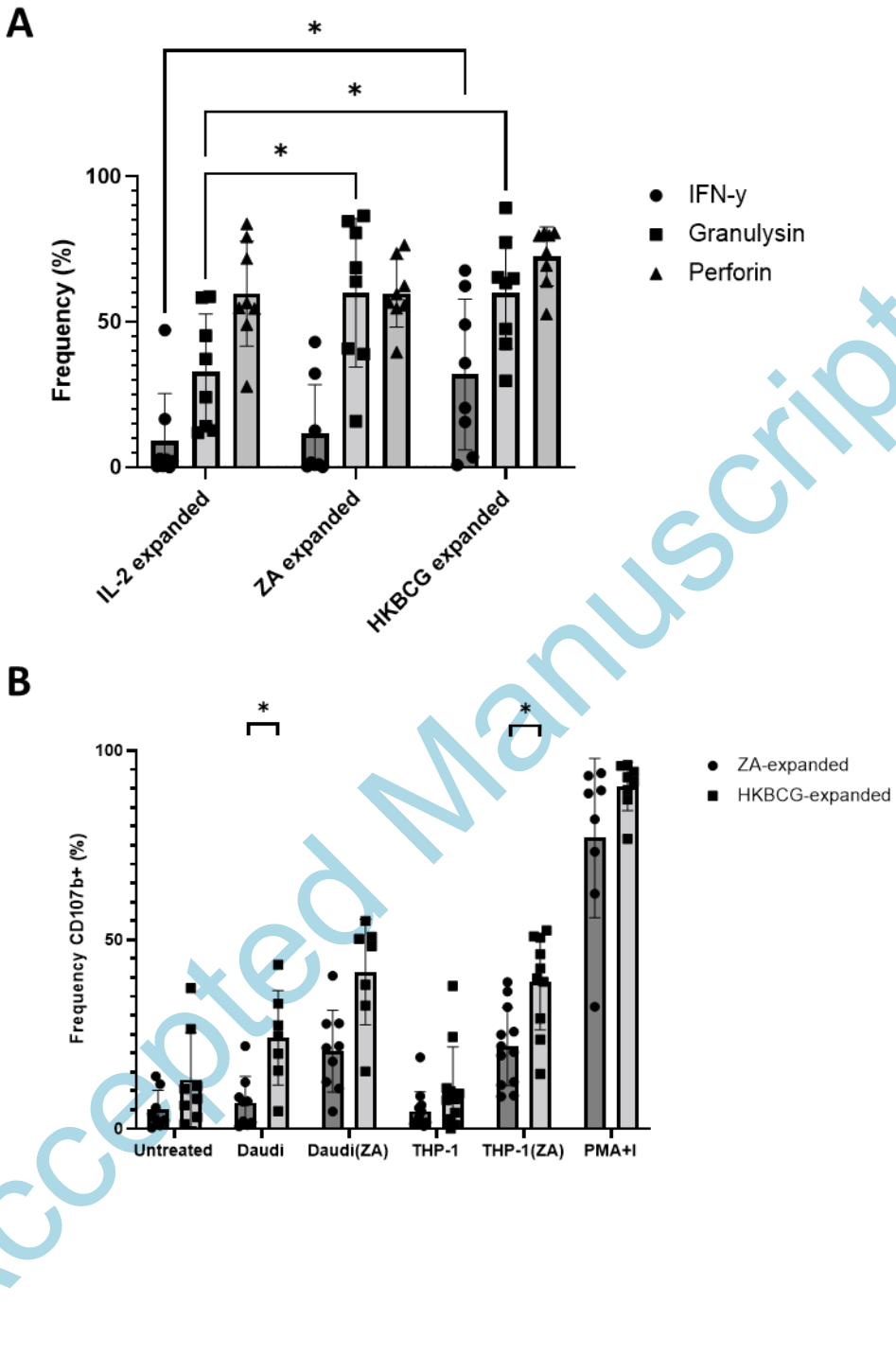

Introduction

Vδ2$^+$ T-cells are the predominant subset of γδ T-cells in human peripheral blood. They express TCR δ chains that use the Vδ2$^+$ arrangement and predominantly pair expression of these δ chains with the Vγ9 γ chain (1). This Vδ2$^+$ TCR arrangement enables these cells to recognise small phosphate antigens (pAgs) via the endogenous pseudo-presenting molecule Butyrophilin 3A1 (BTN3A1) (2–4). Endogenous pAgs occur under homeostatic conditions as intermediates of the mevalonate metabolic pathway which is involved in the production of cholesterol and in the prenylation of proteins. Dysregulation of this pathway occurs in malignantly transformed cells and can result in the accumulation of mevalonate pathway intermediates such as isopentenyl pyrophosphate (IPP) (5). This accumulation can lead to recognition of tumour cells by Vδ2$^+$ cells, supporting a role for Vδ2$^+$ cells in immunosurveillance against tumours (6,7).

Exogenous pAgs are produced by a range of pathogens, including plasmodia and bacteria, and can also be detected by Vδ2$^+$ cells via their Vδ2$^+$ TCR. Mycobacteria, for example, have been shown to use the MEP/DOXP pathway (a prokaryotic analogue of the mevalonate pathway) in which the pAg (E)-4-hydroxy-3-methyl-but-2-enyl pyrophosphate (HMBPP) is produced as an intermediate. HMBPP displays a 30 000-fold higher potency than IPP, inducing proliferation and cytokine production by Vδ2$^+$ cells even at the picomolar range (8). Bacterially derived HMBPP has been shown to render human cells susceptible to recognition and destruction by Vδ2$^+$ cells. As such, Vδ2+ cells have been implicated in immune responses to HMBPP-producing pathogens including *Mycobacterium tuberculosis*, *Listeria monocytogenes* and *Salmonella enterica* (9–11). The ability of Vδ2$^+$ cells to recognise both bacterially infected and malignantly transformed cells raises the question of whether pAg-producing bacteria could be used to manipulate Vδ2$^+$ cell responses in a manner that could facilitate enhanced anti-tumour Vδ2$^+$ cell activity.

The aminobisphosphonate drug Zoledronic acid (ZA) is used routinely in the treatment of osteoporosis and bone degeneration associated with the development of bone metastases (11, 12). It may also have potential as an immunotherapeutic agent. In the context of γδ T-cells, ZA has been shown to inhibit the mevalonate pathway at the level of farnesyl pyrophosphate synthase (FPPS), leading to an accumulation of IPP which results in normally Vδ2$^+$ cell-resistant tumour cells becoming susceptible to recognition and killing by Vδ2$^+$ cells (7). ZA administration both *in vitro* and *in vivo* has been shown to lead to the activation and proliferation of potentially tumour-reactive Vδ2$^+$ cells. Both methods of Vδ2$^+$ cell expansion have been evaluated in clinical trials (14–21).

Bacillus Calmette-Guérin (BCG) is routinely used in the treatment of non-invasive bladder cancer and has also been used intralesionally in the treatment of melanoma (22–24). In both cases, treatment has been associated with favourable clinical responses in cancer patients that appear to be associated with infiltration of various types of immune cell into the site where BCG was administered (25–27). Vδ2$^+$ cells have been shown to be capable of lysis of mycobacterially infected cells, making them candidate mediators of anti-tumour activity induced by BCG treatment (28,29). Supporting this speculation is evidence of infiltration of activated, IFNγ$^+$ Vδ2$^+$ cells into BCG-treated melanoma lesions where their presence was associated with lesion regression (30).

In this study, we investigate potential mechanisms by which BCG could be used to potentiate anti-tumour Vδ2$^+$ cell responses. We show that BCG can be used to induce proliferation of Vδ2$^+$ cells in PBMCs and that the resulting Vδ2$^+$ cell populations produced a more diverse and higher magnitude cytokine response to tumour cells than ZA-expanded Vδ2$^+$ cells. The failure of ZA-expanded cells to respond optimally to tumour target cells was associated with upregulation of exhaustion and inhibitory markers CD57 and PD-1 respectively. *In vivo* studies using the Rhesus macaque model of BCG vaccination show that intradermal BCG vaccination is sufficient to induce expansion of Vδ2$^+$ cells in the peripheral blood. Together, these results suggest that BCG vaccination could be a viable way of promoting the expansion of Vδ2$^+$ cells with enhanced anti-tumour potential and furthermore that BCG or ZA could be used to target Vδ2$^+$ cell responses towards tumour cells.

Materials and methods

PBMC isolation

PBMCs were isolated from anonymised leukocyte cones which were acquired from NHS Blood and Transplant, St. George's, University of London (NHSBT) under ethical approval SGREC16.0009. Contents of leukocyte cones were diluted approximately 1:10 in RPMI 1640 media (Sigma) supplemented with 10% Foetal Bovine Serum (FBS) (Sigma) and PBMCs isolated by density gradient centrifugation using Histopaque-1077 (Sigma). Residual erythrocytes were lysed using RBC lysis buffer (BioLegend) and platelets removed by repeated centrifugation at 200g. PBMCs were re-suspended in freezing medium (45% RPMI-1640, 45% FBS, 10% DMSO) and stored for two days at -80°C before being transferred for storage in liquid nitrogen.

Cell culture

Tumour cell culture

Daudi and THP-1 cells were acquired from the European Collection of Authenticated Cell Cultures (ECACC) (Public Health England, Porton Down). Cell lines were maintained by culturing in RPMI 1640 medium containing 10% FBS at 37 °C with 5% CO_2 and were passaged every 2-4 days to maintain recommended cell densities. Passage numbers were universally kept below 20.

BCG culture

BCG Pasteur strain and GFP-expressing BCG Pasteur strain were kind gifts of Dr Rajko Reljic (St. George's, University of London). Bacterial cells were cultured in 7H9 media (Becton Dickinson) supplemented with 10% Middlebrook ADC enrichment (Sigma) and 0.05% Tween 80 (Sigma) and grown in a shaking incubator at 37°C for four weeks after which cells were washed and re-suspended in 15% glycerol and 85% 7H9 liquid medium and frozen at -80°C in cryogenic vials (Nalgene). Prior to use in assays bacteria were enumerated using a colony forming unit counting method in which bacteria were inoculated onto agar plates containing 7H11 media (Becton Dickinson) supplemented with 10% Middlebrook OADC enrichment (Sigma). Number of visible colonies was determined after three weeks culture at 37°C. In some instances, where indicated, BCG was heat killed at 80°C for 30 minutes prior to culture with PBMCs.

BCG and ZA expansion of $V\delta2^+$ cells

5×10^6 thawed PBMCs/ml were stimulated in round bottomed 96 well plates with 15ng/ml IL-2 (R&D systems) in combination with either 0.5, 1, 5 or 10µM ZA (Sigma) or $2x10^4$ CFU BCG/well. Every 2-3 days, 100µl of culture media was replaced with 100µl fresh media containing 30ng/ml IL-2. Cells were cultured for 12 days before use in downstream applications. In experiments where isolated $V\delta2^+$ cells were used. Expanded cells were re-suspended in MACS buffer (PBS, 0.5% BSA, 2mM EDTA) and isolated using the γδ T-cell negative selection kit - 130-092-892 (Miltenyi Biotec) according to manufacturer's instructions.

Flow cytometry

Surface and intracellular staining

Cells were collected, washed using FACS buffer (PBS (Sigma) containing 1% BSA (Sigma), 0.1% Sodium azide (NaN_3) (Sigma), 2mM Ethylenediaminetetraacetic acid (EDTA) (Sigma)) and stained for 15 minutes at room temperature with fluorescently conjugated antibodies at manufacturer

recommended concentrations. Alternatively, for intracellular staining experiments, cells were re-suspended in 500µl fixation buffer (BioLegend) and incubated for 20 minutes before addition of 500µl 1x permeabilization wash buffer (BioLegend) and two further wash steps with permeabilization wash buffer. Permeabilised cells were stained for 20 minutes at room temperature with fluorescently conjugated antibodies at manufacturer recommended concentrations and washed in permeabilization wash buffer. All stained cells were washed with FACS buffer before being re-suspended in 300µl Cellfix (BD) and acquired using a BD LSRII flow cytometer or LSR Fortessa X20 (both BD biosciences). The following antibodies were used: anti-CD3-Alexafluor 700 (OKT3), anti-CD3-PerCP (OKT3), antiCD69-FITC (FN50), anti-CD107b-PE (H4B4), anti-CD16-PE (3G8), anti-CD57-PE-Cy7 (HNK-1), anti-NKG2D-APC (1D11), anti-granulysin-PE (DH2) all from BioLegend; anti-Vδ2-PerCP-Vio700 (REA771), anti-CD56-VioBright FITC (AF12-7H3), anti-Vδ2-PE (123R3), anti-IFNγ-APC-Vio770 (45-15), anti-perforin-APC (δG9) all from Miltenyi Biotec; anti-Vγ9-FITC (7A5) from Thermo-Fisher Scientific. Data was analysed using FlowJo v10 (BD).

CD107b mobilisation assay

A solution containing 5µl FITC-conjugated CD107b antibody, 5µg/ml Brefeldin A, 2µM Monensin (all BioLegend) and 5µl media was added directly to 200µl effector: target co-cultures at 10µl per well 15 minutes after initiation of co-culture. Cells were incubated for 4 hours before being harvested and stained using the protocol described in 'Flow cytometry' section. 25 ng/ml Phorbol 12-myristate 13-acetate (PMA) and 1µg/ml ionomycin (I) were added to positive control wells prior to addition of monensin and brefeldin.

Cytotoxicity assay

Tumour target cells were prepared by overnight culture of $6x10^5$ cells/ml in the presence of 50µM ZA or BCG at a multiplicity of infection (MOI) of 1. These cells were then labelled for 15 minutes with Cell Trace Far Red (Life technologies) in PBS at manufacturer recommended concentrations, washed twice with RPMI 1640 media supplemented with 10% FBS and added to round bottom 96 well plates at $5x10^4$ cells per well. Expanded, isolated effector cells were added to target cells at a 1:1 effector to target ratio. Cells were co-cultured for 18 hours before being labelled with Live/Dead red stain (Life technologies) in PBS for 20 minutes in the dark at room temperature and acquired using BD LSRII flow cytometer. Specific killing was calculated by subtracting the frequency of dead cells in 'target alone' conditions from the frequency of dead cells in co-culture conditions.

Confocal microscopy

Growing THP-1 cells were washed in culture media and re-suspended at $1x10^6$ cells/ml. Cell suspension was transferred to black flat-bottomed 96 well plates (Corning) at 100µl per well to give $1x10^5$ cells per well. GFP-expressing BCG was thawed, re-suspended to give $1x10^6$ CFU/ml or $5x10^6$ CFU/ml as indicated and added to plates at 100µl per well to give THP-1: BCG bacilli ratios of 1:1 and 1:5 respectively. After 24 hours, cells were washed twice with PBS before being fixed by re-suspension in 4% paraformaldehyde (PFA; Sigma) in the dark at room temperature for 10 minutes. Cells were washed twice with PBS and resuspended in PBS containing 1µg/ml 4', 6-diamidino-2-phenylindole (DAPI). Labelled cells were imaged using a 40x CFI S Plan Fluor ELWD objective lens of a Nikon A1R confocal microscope. A 405nm laser was used to detect DAPI fluorescence (displayed in blue) and 488nm laser used to detect GFP fluorescence (displayed in green). NIS Elements version 4.2 software was used to acquire and analyse data.

Legendplex assay

A Human CD8/NK Panel (BioLegend Cat. No. 740267) multi analyte assay was used to detect proteins secreted during $V\delta2^+$ cell-tumour cell co-culture. The kit was used according to manufacturer's instructions. Specifically, 100µl supernatants were collected from γδ T-cell – tumour cell co-cultures after 24 hours and frozen. Prior to use, supernatants were thawed and centrifuged at 1400g for 5 minutes to remove cell debris. 25µl supernatant plus 25µl assay buffer was added to each well of a 96-well 'V' bottomed plate. A set of eight protein standards were prepared by serial dilution of a cocktail consisting of known concentrations of the recombinant forms of the 13 proteins detected by this kit in assay buffer. 25µl aliquots of these standards plus 25µl culture medium were added to 'standard' wells of the 96 well plate in duplicate. To both sample wells and standard wells, 25µl each of pre-mixed beads and detection antibodies were added before incubating in the dark on a plate shaker at 600rpm at room temperature for 2 hours. 25µl PE-streptavidin was added before incubating on a plate shaker at 600rpm for 30 mins. Plates were washed twice by centrifugation at 1000g for 5 minutes. Samples were transferred to FACS tubes and immediately acquired using a BD LSRII flow cytometer using recommended data acquisition templates provided by BioLegend. FCS files were exported and analysed using LEGENDplex™ data analysis software.

Macaque vaccination and sampling

All macaque studies were conducted in animals housed in compatible social groups and in accordance with the Home Office (UK) Code of Practice for the Housing and Care of Animals Used in Scientific Procedures (1989) and the Guidelines on Primate Accommodation, Care and Use of the

National Committee for Refinement, Reduction and Replacement (NC3Rs), issued in August 2006. All protocols involving animals were approved by the Ethical Review Body of the Public health England, Porton, United Kingdom and were authorized under an appropriate UK Home Office project license. Animals were sourced from an established, closed UK breeding colony, none of the animals had been used previously for experimental procedures (31). Absence of previous exposure to mycobacterial antigens was confirmed by tuberculin skin test as part of colony management procedures and by screening for IFN-γ ELISpot (MabTech, Nacka. Sweden) responses to tuberculin-PPD (purified protein derivative) (SSI, Copenhagen, Denmark), and pooled 15-mer peptides of ESAT6 and CFP10 (Peptide Protein Research LTD, Fareham, UK).

Housing pens were designed to allow access to indoor and outdoor environments and measured approximately 20 m^2 by 2.5 m high for indoor-, and 37.8 m^2 by 3.7 m high for outdoor-enclosures. Pens were constructed with a range of high-level observation balconies and a floor of deep litter was provided in internal enclosures to allow foraging. Additional environmental enrichment was afforded by the provision of toys, swings, climbing apparatus and feeding puzzles for stimulation. In addition to standard old-world primate pellets, diet was further supplemented with a selection of fresh vegetables and fruit. For each procedure, sedation was applied by intramuscular injection with ketamine hydrochloride (10 mg/kg) (Ketaset, Fort Dodge Animal Health Ltd, Southampton, UK).

Six of a cohort of 12 (one male, 11 female) rhesus macaques (*Macaca mulatta*) of Indian origin aged between 14 and 16 years were immunized intradermally in the upper left arm with 100 µl BCG, Danish strain 1331 (SSI, Copenhagen, Denmark). The BCG vaccine was prepared and administered according to the manufacturer's instructions for the preparation of vaccine for administration to human adults; this was done by adding 1 ml Saunton's medium as the diluent to a vial of vaccine to give a suspension of BCG at an estimated concentration of 2×10^6 to 8×10^6 CFU/ml (32). 10 ml blood samples were collected four and six-weeks post vaccination. Peripheral blood mononuclear cells (PBMCs) were isolated from heparin-anticoagulated blood by Ficoll-Hypaque Plus (GE Healthcare, Buckinghamshire, United Kingdom) density-gradient separation using standard procedures as previously described (33).

ELIspot

An IFN-γ enzyme-linked immunosorbent spot (ELISpot) assay was used to determine the numbers of IFN-γ producing mycobacterium-specific T-cells in PBMCs using a human/monkey IFN-γ kit (Mabtech) as described previously (33). In brief, PBMCs were cultured with 10µg/ml purified protein derivative (PPD) (SSI, Copenhagen), or without antigen, in triplicate, and incubated for 18 hours. Phorbol 12-myristate (100 ng/ml) (Sigma) and ionomycin (1µg/ml) (CN Biosciences) were used as a

positive control. After culture, spots were developed according to the manufacturer's instructions. Determinations from triplicate tests were averaged. Data were analysed by subtracting the mean number of spots in medium-only control wells from the mean counts in antigen stimulated wells (32).

Results

BCG causes the activation and proliferation of Vδ2$^+$ cells

In order to address the hypothesis that BCG-primed Vδ2$^+$ cells have anti-tumour activity, initial experiments sought to determine the effect of BCG on Vδ2$^+$ cells in terms of activation state and induction of proliferation. Isolated PBMCs were treated with BCG at a range of CFU values or ZA at a range of concentrations as a control (based on extensive evidence that ZA induced Vδ2$^+$ cell activation and proliferation). Activation of Vδ2$^+$ cells and CD3$^+$Vδ2$^-$ cells was assessed using CD69 expression (Figure 1A). Results show that both BCG and ZA cause activation of Vδ2$^+$ cells in a dose dependent manner (Figure 1B+C). It was observed that at the highest tested CFU values, BCG appeared to induce cell death as assessed by light microscopy and shift in the FSC SSC characteristics of cells as determined by flow cytometry. Similarly, whilst ~100% of Vδ2$^+$ cells were consistently activated by stimulation at 50 and 250 µM ZA, fewer Vδ2$^+$ cells were activated at 1000 µM – likely due to toxicity of the drug at this high concentration (Figure 1C).

Following 12 days stimulation with BCG and ZA PBMCs were stained for expression of Vδ2$^+$ TCR and CD3 enabling Vδ2$^+$ and T-cell populations to be gated and Vδ2$^+$ cell expansion to be assessed. Vδ2$^+$ cell frequencies from 9 donors stimulated with IL-2 alone or IL-2 in combination with 2x10^4 CFU BCG, heat-killed BCG or 1µM ZA. The concentration of ZA chosen induced similar levels of CD69 expression compared to BCG and in addition to induction of CD69 stimulation, 1µM ZA induced high frequencies of Vδ2$^+$ cells compared to IL-2 alone (Figure 1D). A high level of batch variability was seen with 2x10^4 CFU BCG with Figure 1d showing data obtained using a BCG batch that caused high amounts of cell death and lower frequencies of Vδ2$^+$ cells. In comparison, heat killed BCG was subject to lower levels of batch variation and consistently induced robust Vδ2$^+$ cell expansions. HKBCG was therefore used preferentially for subsequent Vδ2$^+$ cell expansions. HKBCG stimulation resulted in higher levels of Vδ2$^+$ cell expansion compared to IL-2 alone, as did stimulation with 1µM ZA (p=0.025 and 0.001 respectively) (Figure 1D).

HKBCG-expanded Vδ2$^+$ cells degranulate in response to tumour cells

Vδ2+ cells are known to exert effector functions via production of IFN-γ, perforin and granulysin (9,34,35). Therefore, we measured the effect of HKBCG and ZA expansion on intracellular expression levels of these molecules. Both ZA and HKBCG expansion caused increased levels of intracellular granulysin expression compared to cells treated with IL-2 alone. In HKBCG-expanded, but not ZA-expanded Vδ2+ cells, intracellular IFN-γ was also upregulated relative to IL-2 only control (Figure 2A).

Having shown accumulation of effector molecules during expansion, we sought to compare the ability of HKBCG-expanded Vδ2+ cells to degranulate in response to tumour target cells to ZA-expanded Vδ2+ cells. HKBCG- or ZA-expanded PBMCs were cultured with tumour cells in the presence of BFA, monensin and anti-CD107b-FITC. The results of these assays show that Vδ2$^+$ cells from HKBCG-expanded cells degranulated more towards Daudi cells and ZA-treated THP-1 cells compared to their ZA-expanded counterparts (p=0.020 and 0.022 respectively) (Figure 2B). Additionally, the results show that ZA treatment of THP-1 cells renders them capable of inducing more degranulation in Vδ2$^+$ cells.

BCG infection of THP-1 cells does not significantly increase their susceptibility to Vδ2$^+$ cell-mediated killing

In order to determine whether BCG-infection could increase susceptibility of tumour cells to lysis by Vδ2$^+$ cells, THP-1 cells were infected with BCG and cultured in the presence of Vδ2$^+$ cells. The BCG infection model used in this series of experiments was characterised using a GFP transformed strain of BCG. Flow cytometry assays showed that after culture in the presence of GFP$^+$BCG, THP-1 cells increased in GFP fluorescence in a BCG dose-dependent manner (Figure 3A+B). To confirm that this increase in fluorescence was associated with true BCG internalisation, confocal microscopy was used to visualise the spatial distribution of bacilli within THP-1 cells (Supplemental Figure 1). Rod-shaped GPF$^+$ bacilli were detected inside THP-1 cells proximal to the nucleus. Infected cells commonly contained multiple bacilli, yet a proportion of cells remained uninfected even after 24 hours, in agreement with the observation using flow cytometry that an upper limit existed in terms of the frequency of infected cells despite increasing BCG CFU values. Infection caused increasing THP-1 cell death with increasing BCG CFU (Supplemental Figure 1). To limit the impact of this effect on future assays a compromise was struck between maximal infection efficacy and minimal cell death induction and an MOI of 1 was selected for assays involving infection of THP-1 cells with BCG.

It was hypothesised that BCG infection of THP-1 cells would be associated with increases in intracellular levels of bacterially derived pAg, HMBPP, and that this would cause Vδ2$^+$ cells to elicit

Vδ2 TCR-dependent killing of BCG-infected THP-1 cells (THP-1(BCG)). To test this hypothesis, ZA- and HKBCG-expanded Vδ2+ cells were enriched using MACS negative selection columns and co-cultured with tumour target cells, including BCG-infected THP-1 cells at a 3:1 ratio. Neither ZA- nor HKBCG-expanded Vδ2$^+$ cells killed THP-1(BCG) cells at significantly higher levels than untreated cells (Figure 3C). In addition to THP-1(BCG) target cells, expanded Vδ2+ cells were cultured with Daudi and THP-1 cells with and without ZA pre-treatment. In multiple pairwise comparisons no significant differences between ZA- and HKBCG-expanded Vδ2+ cell killing of tumour cell targets were observed despite the prior observation of enhanced degranulation towards THP-1 cells by HKBCG-expanded Vδ2+ cells.

ZA- and HKBCG-expanded Vδ2$^+$ produce qualitatively and quantitatively different cytokine responses to tumour cells

Supernatants from Vδ2+ cell cytotoxicity assays were collected and Legendplex assays performed to compare the profiles of effector molecules released by ZA- and HKBCG-expanded Vδ2+ cells upon tumour cell recognition (Figure 4A+B). In order to visualise differences in cytokine profiles between ZA- and HKBCG-expanded cells Z-scoring within individual analytes was performed and scored data plotted as a heatmap (Figure 4C+D). Compared to ZA-expanded Vδ2+ cells, HKBCG-expanded cells tended to release more cytolytic molecules including granzymes and granulysin in response to tumour cell co-culture, whereas ZA-expanded Vδ2+ cells tended towards relatively higher levels of Th2-assocaited cytokines. In comparisons of individual analytes only production of granulysin in response to THP-1 cells was significantly higher in HKBCG-expanded cells as determined by multiple pairwise T-tests after correcting for multiple comparisons ($p=0.03$) (Figure 4E). Together this data characterises HK-BCG-expanded cells as superior cytokine and cytolytic mediator producers compared to ZA-expanded cells.

ZA expansion drives Vδ2+ cells towards an exhausted phenotype that is not observed following HKBCG expansion

We next sought to investigate whether phenotypic differences could account for the increased cytokine-producing potential of HKBCG-expanded Vδ2$^+$ cells. PBMCs from 9 donors were expanded using IL-2, BCG, HKBCG and ZA for 12 days and expression of CD3, Vδ2 TCR, CD16, CD56, NKG2D and CD57 was determined using flow cytometry. Equal numbers of events from each donor and stimulation condition were concatenated and tSNE clustering was employed to agnostically identify clusters of cells that may be differentially associated with different expansion protocols (Figure 5A). Striking differences in the distribution of tSNE clusters were observed between ZA- and HKBCG-

expanded cells (Figure 5B). Specifically, different frequencies of 'cluster 7' events were observed in ZA-expanded Vδ2+ cells compared to HKBGC-expanded cells (Figure 5C). An ANOVA confirmed statistically significant differences in 'cluster 7' frequencies between ZA- and HKBCG-expanded cells ($p<0.0001$). Using individual marker heatmap overlays, 'cluster 7' was identified as Vδ2+ cells expressing high levels of CD57. CD57 has been used as a marker of replicative senescence in $V\delta2^+$ cells (36), suggesting that the differences in cytokine producing potential between ZA- and HKBCG-expanded Vδ2+ cells could be associated with a highly differentiated state or functional exhaustion.

ZA-expanded Vδ2+ cells express high levels of inhibitory checkpoint molecules

Having observed high levels of CD57 expression on ZA-expanded Vδ2+ cells, we sought to determine whether these cells express other markers that may be associated with an exhausted or functionally deficient phenotype. Flow cytometry was used to determine the frequency of expanded Vδ2+ cells expressing various checkpoint molecules after HKBCG and ZA expansion. ZA-expansion caused increasing expression of PD1, TIM3, TIGIT and LAG3 in a dose-dependent manner in Vδ2+ cells (Figure 6A). Interestingly, whilst HKBCG expansion was associated with high levels of TIM3 and LAG3 expression, it was not associated with increased expression of PD1 which remained at levels of expression comparable to Vδ2+ cells expanded by concentrations of ZA as low as 0.5μM. The functional implications of the dose-dependent increases in checkpoint molecule expression caused by ZA were investigated using a cytotoxicity assay. THP-1 cells were co-cultured with Vδ2+ cells expanded using different concentrations of ZA or HKBCG. Concordant with checkpoint molecule expression data, Vδ2+ cells expanded using higher concentrations of ZA were poorer at killing THP-1 cells compared to HKBCG expanded Vδ2+ cells and Vδ2+ cells expanded using low ZA concentrations (Figure 6B). This provides further evidence that ZA-expanded Vδ2+ cells may be associated with a highly differentiated or exhausted phenotype.

Intradermal BCG vaccination of Rhesus macaques causes increases in circulating $V\delta2^+$ cell frequency.

In order to determine the physiological relevance of the finding that BCG is capable of causing expansion of $V\delta2^+$ cells with enhanced anti-tumour activity, six rhesus macaques were vaccinated intradermally with BCG and the frequency of $V\delta2^+$ cells in their peripheral blood measured 4- and 6-weeks post-vaccination. Due to well documented cross reactivity with non-human primate species, the 7A5 Vγ9 clone was selected for these assays over anti-$V\delta2^+$ antibodies using the assumption that almost all circulating $V\gamma9^+$ cells co-express the $V\delta2^+$ delta chain. Intradermal vaccination successfully induced BCG-specific responses in all vaccinated animals as determined using IFN-γ ELISpot which

showed increased responsiveness to subsequent PPD stimulation in PBMCs of all vaccinated animals (Figure 7A). The frequency of circulating Vγ9$^+$ cells was elevated in a subset of vaccinated animals four weeks post BCG vaccination before returning to baseline levels at 6 weeks (Figure 7B). This suggests that delivery of BCG via the same route used as standard in human vaccination can cause an increase in Vδ2$^+$ cell frequency, reminiscent of the results obtained from *in vitro* BCG treatment of human PBMCs (Figure 1D).

PBMCs isolated from blood collected from macaques pre-vaccination and four weeks post vaccination were co-cultured with ZA-pre-treated or untreated tumour cell lines for four hours in the presence of Brefeldin A, monensin and anti-CD107b as previously described for *in vitro*-expanded human Vδ2$^+$ cells. Xenogeneic recognition of human tumour cell lines by macaques Vδ2$^+$ cells occurred at low levels as expected based on non-MHC-dependent mechanism of Vγ9Vδ2 TCR recognition. As in results described with human Vδ2$^+$ cells, macaque Vδ2$^+$ cells degranulated and produced IFN-γ in response to human tumour cells lines and the magnitude of these responses was elevated by pre-treatment of tumour cell lines with ZA (Figure 7C-E). No significant differences were observed between pre-vaccination and post-vaccination Vδ2$^+$ cells in terms of effector responses although a consistent but non-significantly lower level of granulysin expression was observed in Vδ2$^+$ cells from post-vaccination samples. These results provide proof of concept that these xenogeneic assays can be used to assess the effect of *in vivo* BCG vaccination on Vδ2$^+$ cell anti-tumour responses in macaques though higher numbers of replicates are required to make conclusive statements about whether BCG vaccination can affect the anti-tumour potential of circulating Vδ2$^+$ cells.

Discussion

Meta-analysis of gene expression data from ~9,000 tumours has shown that of all leukocyte subsets investigated, high γδ T-cell frequency correlated most closely with favourable disease outcome (37). This finding strongly suggests that γδ T-cells are associated with anti-tumour immunity. Evidence in both this report and others show that the circulating Vδ2$^+$ subset of γδ T-cells exhibit strong anti-tumour responses encompassing direct cytotoxic function and cytokine production (38–43). Despite this data, clinical trials in which Vδ2$^+$ cell-based interventions have been tested in various cancer types have yielded diverse and often disappointing results. The majority of trials aiming to harness the aforementioned anti-tumour potential of Vδ2$^+$ cells *in vivo* have used either phosphoantigens or ZA to do so. Whilst proliferation and differentiation of Vδ2$^+$ cells has been reported in some patients treated with ZA (19,21), not all individuals receiving such treatments undergo measurable changes in

Vδ2$^+$ cell frequency or other characteristics (20) and few benefit from treatment as determined by disease progression. Clearly novel methods of manipulating Vδ2$^+$ cell anti-tumour functions are necessary to realise their potential in cancer therapy.

BCG was investigated in this study as a potential inducer of Vδ2$^+$ cell anti-tumour function based on evidence that it can cause Vδ2$^+$ cell expansions *in vivo* and induces tumouricidal effects in malignancies such as melanoma (30,44,45). Results presented in this study show that *in vitro* BCG treatment of PBMCs leads to proliferation of Vδ2$^+$ cells which exhibit cytotoxic effects towards tumour cell lines. This may be associated with the well documented ability of Vδ2$^+$ cells to recognise both bacteria-derived phosphoantigens such as HMBPP (and other antigens such as mGLP) and endogenous pAgs like IPP which is overexpressed in some tumour cell lines. Previous work from our group has also shown that BCG treatment of PBMCs results in a coordinated response involving CD4$^+$ T-cells and myeloid dendritic cells (mDCs), which causes Vδ2$^+$ cell activation and cytokine production (46). Therefore, multiple mechanisms likely contribute to the activation of tumour-responsive Vδ2$^+$ cells by BCG.

In the work presented in this report, we build on these observations, showing that BCG is capable not only of activation of Vδ2$^+$ cells, but of promoting their expansion and inducing Vδ2$^+$ cells with a sustained and enhanced ability to elicit both cytotoxic and cytokine responses to tumour cells. Moreover, we show that zoledronic acid expansion of Vδ2$^+$ cells generated a population of cells with relatively less robust anti-tumour effector responses in terms of cytokine and cytolytic mediator production compared to BCG expansion.

The mechanisms underlying the improved anti-tumour priming of Vδ2$^+$ cells after BCG expansion compared to ZA expansion remain obscure, but could depend on a number of factors including: the effect of signalling via TLRs or other Vδ2$^+$ PRRs induced by BCG concomitantly with HMBPP-dependent Vγ9Vδ2 TCR signalling; the effect of cytokines generated by PBMCs in response to BCG stimulation priming differential γδ T-cell responses; and the expansion of Vδ2$^+$ cell populations with differing TCR repertoires caused by ZA and BCG expansion resulting in different responses to target cells. Additionally, it could be the case that ZA causes detrimental effects on Vδ2$^+$ cell function for example by inhibition of mevalonate metabolism impeding anti-tumour responses of ZA-expanded Vδ2$^+$ cells.

The suggestion that cytokine production by PBMCs after BCG stimulation could affect subsequent functional characteristics of Vδ2$^+$ cells is based on both observations from our own laboratory that CD4+ T-cell and mDC-mediated IL-12p70 production supports Vδ2$^+$ cell activation and recent

evidence from García-Cuesta et al. supporting the idea that BCG-induced cytokine responses by PBMCs lead to enhanced cytotoxic effects in lymphocyte subsets (46,47). The authors demonstrated that BCG treatment of PBMCs caused proliferation of $CD56^{bright}$ NK cells which were primed to elicit more potent degranulation responses towards tumour target cells. It was suggested that this priming effect was mediated by soluble factors produced by PBMCs in response to BCG. Among others, the authors showed that IL-12p70 IL-1β and IL-23 were produced by BCG stimulated PBMCs, all of which have been shown to modify the cytokine production profile of TCR stimulated $V\delta2^+$ cells (48,49).

Another potential explanation for the observed differences in effector responses between ZA- and BCG-expanded $V\delta2^+$ cell populations could be derived from differential skewing of their clonal diversity. Hoft *et al*. have shown differential distribution of $V\delta2^+$ cell clonotypes in pAg-expanded, compared to mycobacteria-expanded, $V\delta2^+$ cells (50). A narrower range of clonotypes arose after expansion with mycobacteria, which was associated with an enhanced ability to limit mycobacterial growth upon subsequent co-culture with M.tb-infected cells. In subsequent publications, the group used nuclear magnetic resonance, and mass spectrometry to identify 6-O-methylglucose-containing lipopolysaccharides (mGLP) as the major component of mycobacteria necessary to induce expansion of a population of $V\delta2^+$ cells with the ability to inhibit mycobacterial growth (51). $V\delta2^+$ cells expanded using enriched mGLP elicited more potent cytokine responses and produced higher levels of granzyme A in response to BCG-infected DCs compared to HMBPP-expanded or M.tb whole lysate-expanded $V\delta2^+$ cells. This is particularly interesting in the context of data presented in this study which shows that BCG-expanded $V\delta2^+$ cells produced higher concentrations of granzyme A in response to THP-1 and THP-1(ZA) target cells compared to ZA-expanded.

In this study we document the decreased levels of degranulation of ZA expanded $V\delta2^+$ cells as well as their altered cytokine production and increased proliferation. One potential explanation for the detrimental effects of ZA on $V\delta2^+$ cells is the potential of ZA to drive $V\delta2^+$ cells towards an exhausted or senescent phenotype. This is supported by the unique expression of CD57 on ZA-expanded cells and the increased expression of immune checkpoint molecules widely regarded as markers of T-cell exhaustion. NBPs have been documented to decrease circulating γδ T-cells with repetitive stimulation resulting in progressive exhaustion (52). On the other hand, it has been shown that bacterial infection with Salmonella enterica generates $V\delta2^+$ immunity with high level of prolonged expansion and lack of anergy due to overproduction of HMBPP which is more reminiscent of the response to bacterial infection (11). The finding of a cluster of CD57 expressing $V\delta2^+$ cells following expansion with ZA suggests a potential for these cells to be senescent. CD57 has been documented

to be expressed on T-cells and NK cells in the final stages of maturation with reduced ability to proliferate but retention of cytotoxic function (53,54). In Vδ2$^+$ cells the marker was associated with shorter telomee length suggesting a population which had undergone higher levels of proliferation (36). The observation of a CD57 expressing population unique to ZA-expanded Vδ2$^+$ cells could define a subset of senescent cells which could underlie the differences observed between BCG and ZA- expanded Vδ2$^+$ cells in terms of their cytokine production.

Recent data from Ryan *et al*., show that Vδ2$^+$ cells with different dominant phenotypic profiles preferentially produce different cytolytic mediators in response to tumour cells (35). Specifically, different Vδ2$^+$ cell phenotypes post-expansion preferentially produced either granzyme B or granzyme K in responses to tumour cell lines, differentially affecting their ability to lyse a range of tumour cell lines. This raises the possibility that phenotypic skewing of BCG-expanded Vδ2$^+$ cells favoured cytotoxic responses towards cell lines used in the research presented in this study. Another recently appreciated implication of enhanced granulysin production by BCG-expanded Vδ2$^+$ cells is that granulysin could have a role in activation and recruitment of the adaptive immune system (55). More specifically, we have recently published data showing that granulysin, released by Vδ2+ cells, can induce migration and maturation of immature DCs, suggesting the potential for BCG-expanded Vδ2$^+$ cells to more effectively contribute to enhancing tumour antigen presentation by DCs (34). High concentrations of granulysin chemoattracts immature DCs, which can then be matured, in part by granulysin, and mature DCs migrate to lower concentrations. Moreover, the *in vivo* studies presented here show a reduced granulysin content of activated Vδ2$^+$ cells four weeks post BCG vaccination, possibly suggesting release of this molecule over the four weeks between vaccination and testing. In our previous paper we show that granulysin secretion increases from expanded Vδ2$^+$ cells for over 9 days suggesting long term release of this molecule occurs (34).

Observations that intradermal BCG vaccination of Rhesus macaques also induced Vδ2$^+$ cell proliferation suggests that this method of BCG delivery could be sufficient for generation of the cytotoxic BCG-responsive Vδ2$^+$ cell populations observed in the *in vitro* experiments performed. Supporting this assertion, Yang *et al.* have shown that intradermal vaccination with BCG followed by subsequent intralesional administration of BCG in melanoma is associated with regression of lesions and concurrent increases in Vδ2$^+$ cell presence in lesions that visibly regressed (30). Interestingly, the authors showed that non-BCG injected lesions proximal to the injected lesions also regressed and that this regression was associated with the presence of γδ T-cells. Future work will aim to address this question by further characterising the responses of *in vivo* BCG-expanded Vδ2$^+$ cells towards tumour cells.

Overall, the results presented in this report represent novel evidence supporting the principle that BCG could be used therapeutically to prime anti-tumour Vδ2$^+$ cell responses. Specifically, results support the assertion that BCG could promote the expansion of Vδ2$^+$ cells with superior cytolytic and cytokine-producing potential compared to ZA-mediated expansion which potential results in cells with a more senescent or exhausted phenotype. Moreover, the results presented show that ZA-treatment of tumour cell targets increases their susceptibility to BCG-expanded Vδ2$^+$ cell lysis. Together these findings argue for possible treatment modalities in which priming doses of BCG are used to promote Vδ2$^+$ cell activation and expansion followed by ZA treatment, ideally at tumour site to enhance targeting of Vδ2$^+$ anti-tumour responses.

Acknowledgements:

We thank the staff of the UKHSA macaque colony for assistance in conducting animal studies and all human volunteers who kindly provided samples.

Ethical Approval:

Human PBMCs used in this work were isolated from anonymised leukocyte cones under St George's Research Ethics Committee approval (SGREC16.0009). Non-human primate work was approved by Public Health England ethical review board and conducted in accordance with Home Office (UK) Code of Practice for the Housing and Care of Animals Used in Scientific Procedures (1989), the Guidelines on Primate Accommodation, Care and Use of the National Committee for Refinement, Reduction and Replacement (NC3Rs) as well as ARRIVE 2.0 guidelines.

Conflicts of interest:

The authors declare no financial or commercial conflicts of interest.

Funding:

All work shown was funded by the Institute for Cancer Vaccines and Immunotherapy (ICVI) (Award number: PhD2015/21) and UK Health Security Agency.

Data Availability:

The data underlying this article will be shared on reasonable request to the corresponding author.

Author contributions:

The authors contributed to this manuscript as follows: Study conception and design: JF, LR, AD, RR, SS, MBS. Generation and interpretation of data using human samples: JF, LR; Generation and interpretation of data using NHP samples: AW, CS, MD, SS, JF, LR. Manuscript preparation: JF, LR, MBS.

References:

1. Bottino C, Tambussi G, Ferrini S, Ciccone E, Varese P, Mingari MC, et al. Two subsets of human T lymphocytes expressing gamma/delta antigen receptor are identifiable by monoclonal antibodies directed to two distinct molecular forms of the receptor. J Exp Med [Internet]. 1988 Aug 1;168(2):491–505. Available from: https://pubmed.ncbi.nlm.nih.gov/2970517

2. Harly C, Guillaume Y, Nedellec S, Peigné C-M, Mönkkönen H, Mönkkönen J, et al. Key implication of CD277/butyrophilin-3 (BTN3A) in cellular stress sensing by a major human γδ T-cell subset. Blood [Internet]. 2012/07/05. 2012 Sep 13;120(11):2269–79. Available from: https://pubmed.ncbi.nlm.nih.gov/22767497

3. Vavassori S, Kumar A, Wan GS, Ramanjaneyulu GS, Cavallari M, El Daker S, et al. Butyrophilin 3A1 binds phosphorylated antigens and stimulates human γδ T cells. Nat Immunol [Internet]. 2013;14(9):908–16. Available from: https://doi.org/10.1038/ni.2665

4. Rigau M, Ostrouska S, Fulford TS, Johnson DN, Woods K, Ruan Z, et al. Butyrophilin 2A1 is essential for phosphoantigen reactivity by γδ T cells. Science. 2020 Feb;367(6478).

5. Bürk MR, Mori L, de Libero G. Human Vγ9-Vδ2 cells are stimulated in a crossreactive fashion by a variety of phosphorylated metabolites. Eur J Immunol [Internet]. 1995 Jul 1;25(7):2052–8. Available from: https://doi.org/10.1002/eji.1830250737

6. Gober H-J, Kistowska M, Angman L, Jenö P, Mori L, De Libero G. Human T cell receptor gammadelta cells recognize endogenous mevalonate metabolites in tumor cells. J Exp Med [Internet]. 2003 Jan 20;197(2):163–8. Available from: https://pubmed.ncbi.nlm.nih.gov/12538656

7. Mattarollo SR, Kenna T, Nieda M, Nicol AJ. Chemotherapy and zoledronate sensitize solid tumour cells to Vgamma9Vdelta2 T cell cytotoxicity. Cancer Immunol Immunother [Internet]. 2007 Aug;56(8):1285—1297. Available from: https://doi.org/10.1007/s00262-007-0279-2

8. Puan K-J, Jin C, Wang H, Sarikonda G, Raker AM, Lee HK, et al. Preferential recognition of a microbial metabolite by human Vγ2Vδ2 T cells. Int Immunol [Internet]. 2007 May 1;19(5):657–73. Available from: https://doi.org/10.1093/intimm/dxm031

9. Meraviglia S, El Daker S, Dieli F, Martini F, Martino A. γδ T cells cross-link innate and adaptive immunity in Mycobacterium tuberculosis infection. Clin Dev Immunol [Internet].

2011;2011:587315. Available from: https://europepmc.org/articles/PMC3022180

10. Frencher JT, Shen H, Yan L, Wilson JO, Freitag NE, Rizzo AN, et al. HMBPP-deficient Listeria mutant immunization alters pulmonary/systemic responses, effector functions, and memory polarization of Vγ2Vδ2 T cells. J Leukoc Biol [Internet]. 2014 Dec;96(6):957—967. Available from: https://europepmc.org/articles/PMC4226791

11. Workalemahu G, Wang H, Puan K-J, Nada MH, Kuzuyama T, Jones BD, et al. Metabolic engineering of Salmonella vaccine bacteria to boost human Vγ2Vδ2 T cell immunity. J Immunol [Internet]. 2014/06/18. 2014 Jul 15;193(2):708–21. Available from: https://pubmed.ncbi.nlm.nih.gov/24943221

12. Major P. The Use of Zoledronic Acid, a Novel, Highly Potent Bisphosphonate, for the Treatment of Hypercalcemia of Malignancy. Oncologist [Internet]. 2002 Dec 1;7(6):481–91. Available from: https://doi.org/10.1634/theoncologist.7-6-481

13. Sunyecz JA. Zoledronic acid infusion for prevention and treatment of osteoporosis. Int J Womens Health [Internet]. 2010 Oct 14;2:353–60. Available from: https://pubmed.ncbi.nlm.nih.gov/21151682

14. Abe Y, Muto M, Nieda M, Nakagawa Y, Nicol A, Kaneko T, et al. Clinical and immunological evaluation of zoledronate-activated Vgamma9gammadelta T-cell-based immunotherapy for patients with multiple myeloma. Exp Hematol. 2009 Aug;37(8):956–68.

15. Nakajima J, Murakawa T, Fukami T, Goto S, Kaneko T, Yoshida Y, et al. A phase I study of adoptive immunotherapy for recurrent non-small-cell lung cancer patients with autologous gammadelta T cells. Eur J cardio-thoracic Surg Off J Eur Assoc Cardio-thoracic Surg. 2010 May;37(5):1191–7.

16. Nicol AJ, Tokuyama H, Mattarollo SR, Hagi T, Suzuki K, Yokokawa K, et al. Clinical evaluation of autologous gamma delta T cell-based immunotherapy for metastatic solid tumours. Br J Cancer [Internet]. 2011;105(6):778–86. Available from: https://doi.org/10.1038/bjc.2011.293

17. Sakamoto M, Nakajima J, Murakawa T, Fukami T, Yoshida Y, Murayama T, et al. Adoptive Immunotherapy for Advanced Non-small Cell Lung Cancer Using Zoledronate-expanded γδ T Cells: A Phase I Clinical Study. J Immunother [Internet]. 2011;34(2). Available from: https://journals.lww.com/immunotherapy-journal/Fulltext/2011/03000/Adoptive_Immunotherapy_for_Advanced_Non_small_Cell.10.aspx

18. Dieli F, Gebbia N, Poccia F, Caccamo N, Montesano C, Fulfaro F, et al. Induction of γδ T-lymphocyte effector functions by bisphosphonate zoledronic acid in cancer patients in vivo. Blood [Internet]. 2003 Sep 15;102(6):2310–1. Available from: https://doi.org/10.1182/blood-2003-05-1655

19. Dieli F, Vermijlen D, Fulfaro F, Caccamo N, Meraviglia S, Cicero G, et al. Targeting human {gamma}delta} T cells with zoledronate and interleukin-2 for immunotherapy of hormone-refractory prostate cancer. Cancer Res [Internet]. 2007 Aug 1;67(15):7450–7. Available from: https://pubmed.ncbi.nlm.nih.gov/17671215

20. Lang JM, Kaikobad MR, Wallace M, Staab MJ, Horvath DL, Wilding G, et al. Pilot trial of interleukin-2 and zoledronic acid to augment γδ T cells as treatment for patients with refractory renal cell carcinoma. Cancer Immunol Immunother [Internet]. 2011/06/07. 2011 Oct;60(10):1447–60. Available from: https://pubmed.ncbi.nlm.nih.gov/21647691

21. Meraviglia S, Eberl M, Vermijlen D, Todaro M, Buccheri S, Cicero G, et al. In vivo manipulation of Vgamma9Vdelta2 T cells with zoledronate and low-dose interleukin-2 for immunotherapy of advanced breast cancer patients. Clin Exp Immunol [Internet]. 2010/05/10. 2010 Aug;161(2):290–7. Available from: https://pubmed.ncbi.nlm.nih.gov/20491785

22. Morton DL, Eilber FR, Holmes EC, Hunt JS, Ketcham AS, Silverstein MJ, et al. BCG immunotherapy of malignant melanoma: summary of a seven-year experience. Ann Surg [Internet]. 1974 Oct;180(4):635–43. Available from: https://pubmed.ncbi.nlm.nih.gov/4412271

23. Guallar-Garrido S, Julián E. Bacillus Calmette-Guérin (BCG) Therapy for Bladder Cancer: An Update. ImmunoTargets Ther. 2020 Feb;9:1–11.

24. A. M, D. E, A.W. B. Intracavitary Bacillus Calmette-guerin in the Treatment of Superficial Bladder Tumors. J Urol. 1976 Aug;116(2):180–2.

25. Honda S, Sakamoto Y, Fujime M, Kitagawa R. Immunohistochemical Study of Tumor-Infiltrating Lymphocytes Before and After Intravesical Bacillus Calmette-Guérin Treatment for Superficial Bladder Cancer. Int J Urol [Internet]. 1997 Jan 1;4(1):68–73. Available from: https://doi.org/10.1111/j.1442-2042.1997.tb00143.x

26. TAN JKL, HO VC. Pooled Analysis of the Efficacy of Bacille Calmette-Guerin (BCG) Immunotherapy in Malignant Melanoma. J Dermatol Surg Oncol [Internet]. 1993 Nov 1;19(11):985–90. Available from: https://doi.org/10.1111/j.1524-4725.1993.tb00989.x

27. Cordova A, Toia F, La Mendola C, Orlando V, Meraviglia S, Rinaldi G, et al. Characterization of human γδ T lymphocytes infiltrating primary malignant melanomas. PLoS One. 2012/11/26. 2012;7(11):e49878–e49878.

28. Dieli F, Ivanyi J, Marsh P, Williams A, Naylor I, Sireci G, et al. Characterization of lung gamma delta T cells following intranasal infection with Mycobacterium bovis bacillus Calmette-Guérin. J Immunol. 2003 Jan;170(1):463–9.

29. Martino A, Casetti R, Sacchi A, Poccia F. Central Memory Vγ9Vδ2 T Lymphocytes Primed and Expanded by Bacillus Calmette-Guérin-Infected Dendritic Cells Kill Mycobacterial-Infected Monocytes. J Immunol [Internet]. 2007 Sep 1;179(5):3057 LP – 3064. Available from: http://www.jimmunol.org/content/179/5/3057.abstract

30. Yang J, Jones MS, Ramos RI, Chan AA, Lee AF, Foshag LJ, et al. Insights into Local Tumor Microenvironment Immune Factors Associated with Regression of Cutaneous Melanoma Metastases by Mycobacterium bovis Bacille Calmette-Guérin. Front Oncol [Internet]. 2017 Apr 5;7:61. Available from: https://pubmed.ncbi.nlm.nih.gov/28424760

31. Rhodes SJ, Sarfas C, Knight GM, White A, Pathan AA, McShane H, et al. Using Data from Macaques To Predict Gamma Interferon Responses after Mycobacterium bovis BCG Vaccination in Humans: a Proof-of-Concept Study of Immunostimulation/Immunodynamic Modeling Methods. Clin Vaccine Immunol [Internet]. 2017 Mar 6;24(3):e00525-16. Available from: https://pubmed.ncbi.nlm.nih.gov/28077441

32. White AD, Sibley L, Dennis MJ, Gooch K, Betts G, Edwards N, et al. Evaluation of the Safety and Immunogenicity of a Candidate Tuberculosis Vaccine, MVA85A, Delivered by Aerosol to the Lungs of Macaques. Clin Vaccine Immunol [Internet]. 2013 May 1;20(5):663 LP – 672. Available from: http://cvi.asm.org/content/20/5/663.abstract

33. Sharpe SA, McShane H, Dennis MJ, Basaraba RJ, Gleeson F, Hall G, et al. Establishment of an aerosol challenge model of tuberculosis in rhesus macaques and an evaluation of endpoints for vaccine testing. Clin Vaccine Immunol [Internet]. 2010 Aug;17(8):1170—1182. Available from: https://europepmc.org/articles/PMC2916246

34. Sparrow EL, Fowler DW, Fenn J, Caron J, Copier J, Dalgleish AG, et al. The cytotoxic molecule granulysin is capable of inducing either chemotaxis or fugetaxis in dendritic cells depending on maturation: a role for Vδ2+ γδ T cells in the modulation of immune response to tumour? Immunology [Internet]. 2020 Aug 13;n/a(n/a). Available from:

https://doi.org/10.1111/imm.13248

35. Ryan PL, Sumaria N, Holland CJ, Bradford CM, Izotova N, Grandjean CL, et al. Heterogeneous yet stable Vδ2(+) T-cell profiles define distinct cytotoxic effector potentials in healthy human individuals. Proc Natl Acad Sci U S A [Internet]. 2016 Dec;113(50):14378—14383. Available from: https://europepmc.org/articles/PMC5167212

36. Xu W, Monaco G, Wong EH, Tan WLW, Kared H, Simoni Y, et al. Mapping of γ/δ T cells reveals Vδ2+ T cells resistance to senescence. EBioMedicine [Internet]. 2019;39:44–58. Available from: http://www.sciencedirect.com/science/article/pii/S2352396418305577

37. Gentles AJ, Newman AM, Liu CL, Bratman S V, Feng W, Kim D, et al. The prognostic landscape of genes and infiltrating immune cells across human cancers. Nat Med [Internet]. 2015/07/20. 2015 Aug;21(8):938–45. Available from: https://pubmed.ncbi.nlm.nih.gov/26193342

38. Dunne MR, Mangan BA, Madrigal-Estebas L, Doherty DG. Preferential Th1 cytokine profile of phosphoantigen-stimulated human Vγ9Vδ2 T cells. Mediators Inflamm [Internet]. 2010;2010:704941. Available from: https://europepmc.org/articles/PMC3043297

39. Gao Y, Yang W, Pan M, Scully E, Girardi M, Augenlicht LH, et al. Gamma delta T cells provide an early source of interferon gamma in tumor immunity. J Exp Med [Internet]. 2003 Aug 4;198(3):433–42. Available from: https://pubmed.ncbi.nlm.nih.gov/12900519

40. Li H, Luo K, Pauza CD. TNF-alpha is a positive regulatory factor for human Vgamma2 Vdelta2 T cells. J Immunol [Internet]. 2008 Nov 15;181(10):7131–7. Available from: https://pubmed.ncbi.nlm.nih.gov/18981134

41. Dhar S, Chiplunkar S V. Lysis of aminobisphosphonate-sensitized MCF-7 breast tumor cells by Vγ9Vδ2 T cells. Cancer Immun [Internet]. 2010 Nov 12;10:10. Available from: https://pubmed.ncbi.nlm.nih.gov/21069948

42. Todaro M, D'Asaro M, Caccamo N, Iovino F, Francipane MG, Meraviglia S, et al. Efficient killing of human colon cancer stem cells by gammadelta T lymphocytes. J Immunol. 2009 Jun;182(11):7287–96.

43. Viey E, Fromont G, Escudier B, Morel Y, Da Rocha S, Chouaib S, et al. Phosphostim-Activated γδ T Cells Kill Autologous Metastatic Renal Cell Carcinoma. J Immunol [Internet]. 2005 Feb 1;174(3):1338 LP – 1347. Available from:

http://www.jimmunol.org/content/174/3/1338.abstract

44. Dieli F, Ivanyi J, Marsh P, Williams A, Naylor I, Sireci G, et al. Characterization of Lung γδ T Cells Following Intranasal Infection with Mycobacterium bovis Bacillus Calmette-Guérin. J Immunol [Internet]. 2003 Jan 1;170(1):463 LP – 469. Available from: http://www.jimmunol.org/content/170/1/463.abstract

45. Shen Y, Zhou D, Qiu L, Lai X, Simon M, Shen L, et al. Adaptive immune response of Vgamma2Vdelta2+ T cells during mycobacterial infections. Science [Internet]. 2002 Mar 22;295(5563):2255–8. Available from: https://pubmed.ncbi.nlm.nih.gov/11910108

46. Fowler DW, Copier J, Wilson N, Dalgleish AG, Bodman-Smith MD. Mycobacteria activate γδ T-cell anti-tumour responses via cytokines from type 1 myeloid dendritic cells: a mechanism of action for cancer immunotherapy. Cancer Immunol Immunother [Internet]. 2011/10/15. 2012 Apr;61(4):535–47. Available from: https://pubmed.ncbi.nlm.nih.gov/22002242

47. García-Cuesta EM, Esteso G, Ashiru O, López-Cobo S, Álvarez-Maestro M, Linares A, et al. Characterization of a human anti-tumoral NK cell population expanded after BCG treatment of leukocytes. Oncoimmunology [Internet]. 2017;6(4):e1293212. Available from: https://europepmc.org/articles/PMC5414876

48. Wesch D, Glatzel A, Kabelitz D. Differentiation of resting human peripheral blood gamma delta T cells toward Th1- or Th2-phenotype. Cell Immunol [Internet]. 2001 Sep;212(2):110—117. Available from: https://doi.org/10.1006/cimm.2001.1850

49. Ness-Schwickerath KJ, Jin C, Morita CT. Cytokine requirements for the differentiation and expansion of IL-17A- and IL-22-producing human Vgamma2Vdelta2 T cells. J Immunol [Internet]. 2010 Jun;184(12):7268—7280. Available from: https://europepmc.org/articles/PMC2965829

50. Spencer CT, Abate G, Blazevic A, Hoft DF. Only a subset of phosphoantigen-responsive gamma9delta2 T cells mediate protective tuberculosis immunity. J Immunol [Internet]. 2008 Oct 1;181(7):4471–84. Available from: https://pubmed.ncbi.nlm.nih.gov/18802050

51. Xia M, Hesser DC, De P, Sakala IG, Spencer CT, Kirkwood JS, et al. A Subset of Protective γ9δ2 T Cells Is Activated by Novel Mycobacterial Glycolipid Components. Infect Immun. 2016 Sep;84(9):2449–62.

52. Rossini M, Adami S, Viapiana O, Fracassi E, Ortolani R, Vella A, et al. Long-Term Effects of

Amino-Bisphosphonates on Circulating γδ T Cells. Calcif Tissue Int [Internet]. 2012;91(6):395–9. Available from: https://doi.org/10.1007/s00223-012-9647-9

53. Kared H, Martelli S, Ng TP, Pender SLF, Larbi A. CD57 in human natural killer cells and T-lymphocytes. Cancer Immunol Immunother. 2016 Apr;65(4):441–52.

54. Brenchley JM, Karandikar NJ, Betts MR, Ambrozak DR, Hill BJ, Crotty LE, et al. Expression of CD57 defines replicative senescence and antigen-induced apoptotic death of CD8+ T cells. Blood. 2003 Apr;101(7):2711–20.

55. Sparrow E, Bodman-Smith MD. Granulysin: The attractive side of a natural born killer. Immunol Lett [Internet]. 2020;217:126–32. Available from: http://www.sciencedirect.com/science/article/pii/S0165247819303499

Figures:

Figure 1

PBMCs were thawed and plated at 5x105 cells per well of round bottomed 96 well plates and stimulated with ZA or BCG at the indicated concentrations for 12 days. Vδ2+ cells responses were assessed using flow cytometry with CD69 staining as a marker of activation and expansion determined by frequencies of Vδ2+ cells as a percentage of live cells. A. Gating strategy used to identify CD69 positive CD3+Vδ2- and CD3+Vδ2+ cells. Example cells from one donor stimulated with 2x104 CFU BCG. B. Stimulation assay conducted for a range of BCG CFU numbers (N=5. Bars represent means ±SD). C. Similar assays conducted using a range of ZA concentrations (N=3. Bars represent means ±SD). D. Vδ2+ cell frequencies were assessed in PBMCs following 12 days under a number of stimulation conditions including 15ng/ml IL-2 alone, 15ng/ml IL-2 with 2x104 CFU BCG or heat killed BCG or 1µM ZA based on results shown in 2.1 B and C. (N=9. Bars represent means ±SD. Repeated measures ANOVA with Geisser-Greenhouse correction and Tukey's multiple comparison test *p<0.05, **p<0.01, ***p<0.001).

Figure 2

PBMCs from eight donors were expanded using either 15ng/ml IL-2 with 1µM ZA or 2x104 CFU heat-killed BCG. After 12 days cells were stained and analysed using flow cytometry. Vδ2+ cells were gated based on FSC SSC characteristics and double positivity for Vδ2-PerCPVio770 and CD3-AF700. A. ICS was used to determine post-expansion frequency of Vδ2+ cells expressing IFN-γ and cytolytic mediators granulysin and perforin. (N=8. Bars represent means ±SD. Two way ANOVA with full fit model and Tukey's multiple comparison *p<0.05)

B. Daudi and THP-1 tumour cells were cultured overnight with or without 50 µM ZA. 5x105 expanded PBMCs were co-cultured with tumour target cells at a 10:1 PBMC: tumour cell ratio for 4.5 hours in the presence of anti-CD107b-FITC antibody, monensin and brefeldin A. (N=12. Bars represent means ±SD. Multiple paired T-tests with Sidak-Bonferroni correction for multiple comparisons *p<0.05).

Figure 3

GFP transfected BCG was cultured overnight with 1x105 THP-1 cells at a range of CFU values. A. a representative plot displaying the gating strategy used to identify live 'infected' THP-1 cells based on GFP and Zombie NIR fluorescence. B. The gating strategy displayed in Figure 3A was applied to determine the percentage of successfully infected THP-1 cells after overnight culture with BCG at a

range of CFU values. C. ZA-expanded Vδ2+ cells were isolated using MACS negative isolation and cultured overnight with 5x104 CTFR-labelled target cells at a 3:1 effector: target cell ratio. Daudi and THP-1 target cells were cultured overnight either with or without 50μM ZA or 1x105 CFU BCG prior to initiation of co-culture. >5000 CTFR+ cells were acquired using a BD LSR Fortessa X20 flow cytometer. Target cells were gated based on CTFR positivity. Specific killing was calculated by subtracting the frequency of dead target cells (as determined by Live/Dead red positive staining) in target alone conditions from the frequency of dead cells in co-culture conditions. (N=12. Bars represent means ± SD Multiple paired T-tests with Sidak-Bonferroni correction for multiple comparisons).

Figure 4

PBMCs from five donors were expanded using 15ng/ml IL-2 with either 1 μM ZA or 2x104 CFU heat-killed BCG/well for 12 days. 5x104 ZA- or heat-killed BCG-expanded MACS-isolated Vδ2+ cells were co-cultured at a 1:1 effector: target ratio for 18 hours with THP-1, THP-1(ZA) or THP-1(BCG) cells. Co-culture supernatants were used in Legendplex assays, with analysis performed using Biolegend LEGENDplex software. A-B. Heat maps displaying mean ng/ml analyte concentrations . C-D. Heat maps displaying z-scores for each analyte. E. Concentrations of IFN-γ, granulysin, IL-17 , granzyme A, granzyme B and TNF-α are shown for assays conducted using expanded and isolated Vδ2+ cells (N=5. Bars represent means ±SD Multiple paired T-tests with Sidak-Bonferroni correction for multiple comparisons *p<0.05).

Figure 5.

PBMCs from nine donors were expanded using 15ng/ml IL-2 with either 1 μM ZA or 2x104 CFU heat-killed BCG/well. After 12 days cells were stained and analysed using flow cytometry. Vδ2+ cells were gated based on FSC SSC characteristics and double positivity for Vδ2 PerCPVio770 and CD3 AF700. Cells were assessed in terms of expression of CD16, CD56, CD57 and NKG2D. A. Equal numbers of events from each donor and each stimulation condition were concatenated and tSNE dimensionality reduction performed. Cell clusters were manually identified and gated. Heat map overlays represent level of expression of each marker independently B. Density plots showing cell distribution by stimulation condition. Each plot represents concatenated data from 9 donors . C. Graph showing frequency of cluster 7 (C7 in Figure 5A) cells according to stimulation condition. (n=9. Bars represent means ±SD. Repeated measures ANOVA with Geisser-Greenhouse correction and Tukey's multiple comparison ***p<0.001, ****p<0.0001).

Figure 6.

PBMCs from four donors were expanded using 15ng/ml IL-2 with either 10, 5, 1 or 0.5 µM ZA or 2x104 CFU heat-killed BCG/well. After 12 days cells were stained and analysed using flow cytometry. Vδ2+ cells were gated based on FSC SSC characteristics and double positivity for Vδ2 PerCPVio770 and CD3 AF700. A. Frequency of PD1, TIGIT, TIM3 and LAG3 positive Vδ2 cells (%) is shown. (N=4. Bars represent means ±SD. For each analyte, repeated measures ANOVA with Geisser-Greenhouse correction and Tukey's multiple comparison test was performed with individual variances computed for each comparison *p<0.05). B. ZA and heat killed BCG-expanded Vδ2+ cells were isolated using MACS negative isolation and cultured overnight with 5x104 CTFR-labelled target cells at a 3:1 effector: target cell ratio. THP-1 target cells were cultured overnight either with or without 50µM ZA or 1x105 CFU BCG prior to initiation of co-culture. >5000 CTFR+ cells were acquired using a BD LSR Fortessa X20 flow cytometer. Target cells were gated based on CTFR positivity. Specific killing was calculated by subtracting the frequency of dead target cells (as determined by Live/Dead red positive staining) in target alone conditions from the frequency of dead cells in co-culture conditions. (N=12. Bars represent means ± SD Repeated measures ANOVA with Geisser-Greenhouse correction and Tukey's multiple comparison *p<0.05).

Figure 7

Phenotypic and functional characteristics of PBMCs obtained from repeated blood sampling of six BCG-vaccinated Rhesus macaques (blue) and six non-vaccinated macaques (red) A. The IFN-γ response to BCG vaccination was measured using ELIspot. PBMCs were stimulated with 10 µg/ml purified protein derivative (PPD) (SSI, Copenhagen). Shown are numbers of IFN-γ spot forming units per 106 PBMCs. B. The frequency of Vγ9+ cells as a percentage of all CD3+ cells from 6 vaccinated individuals (blue) and 6 non-vaccinated individuals (red) determined using flow cytometry. C – E. PBMCs from 6 BCG-vaccinated macaques collected pre- and 4 weeks post BCG vaccination were co-cultured with the indicated target cells at an effector: target ratio of 10:1 for 4.5 hours in the presence of anti-CD107b antibody, monensin and brefeldin A. Plots show frequencies of Vδ2+ cells expressing CD107b, granulysin and IFN-γ. (N=6. Bars represent means ± SD. Multiple paired T-tests with Sidak-Bonferroni correction for multiple comparisons).

Figure 1

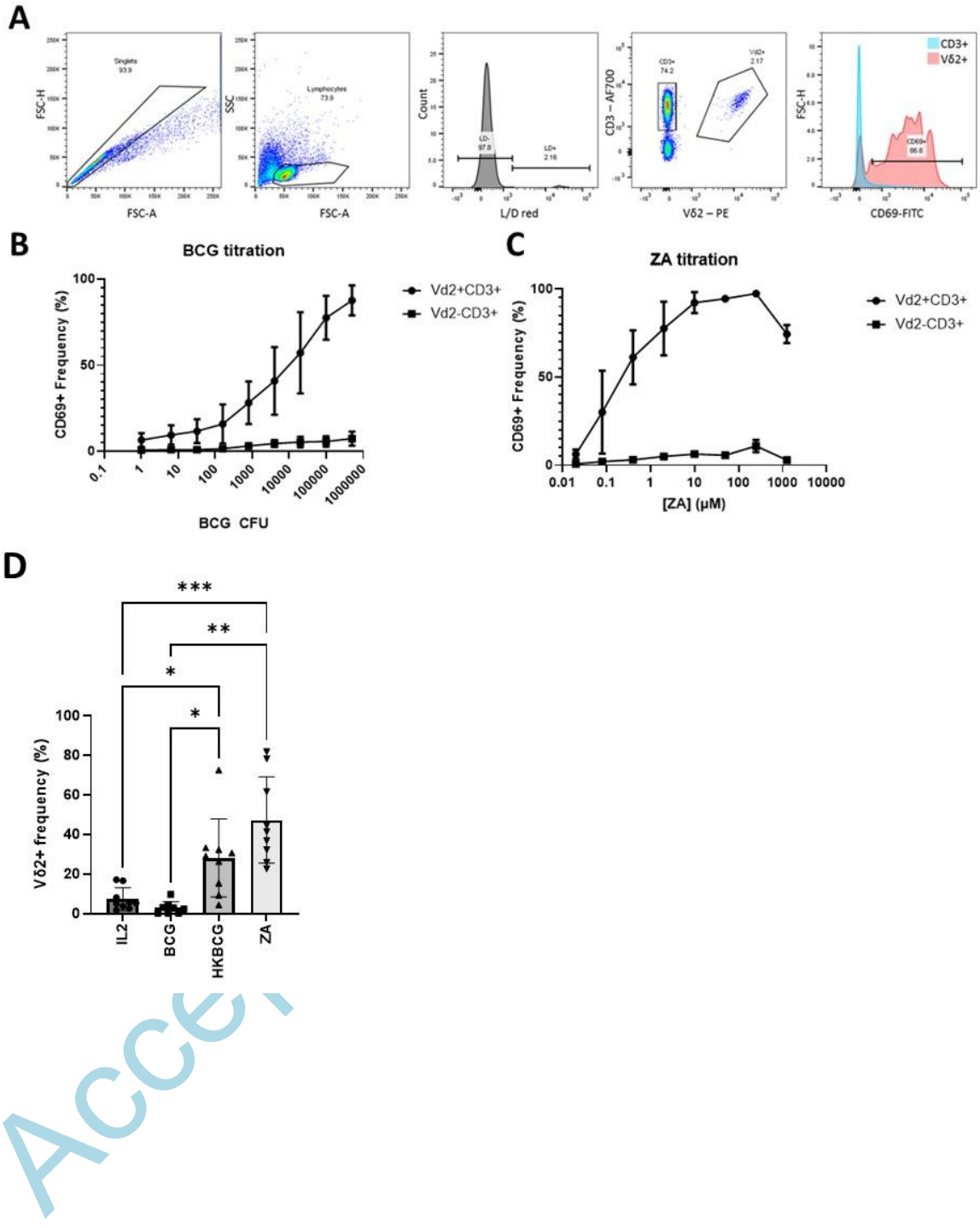

Figure 2

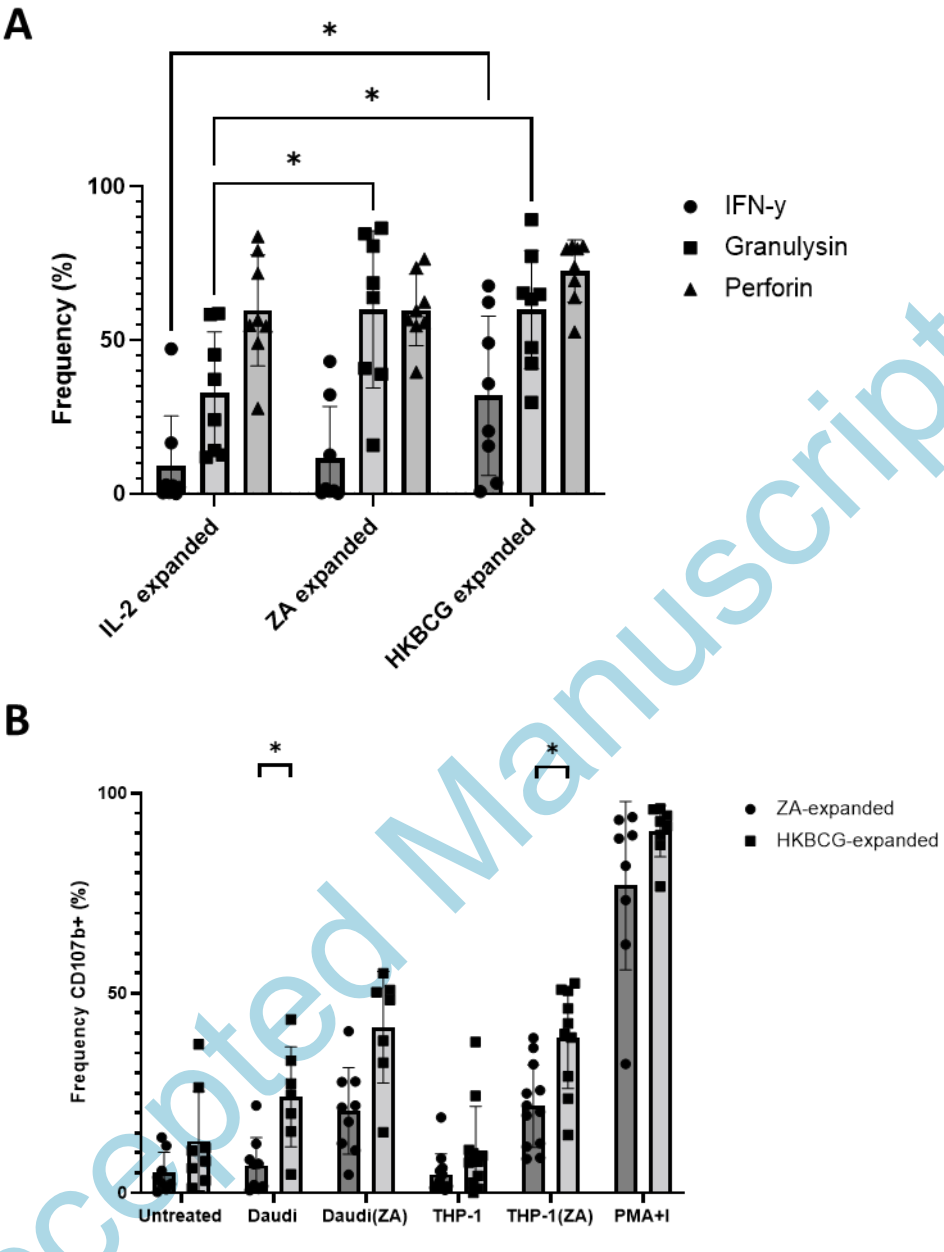

Figure 3

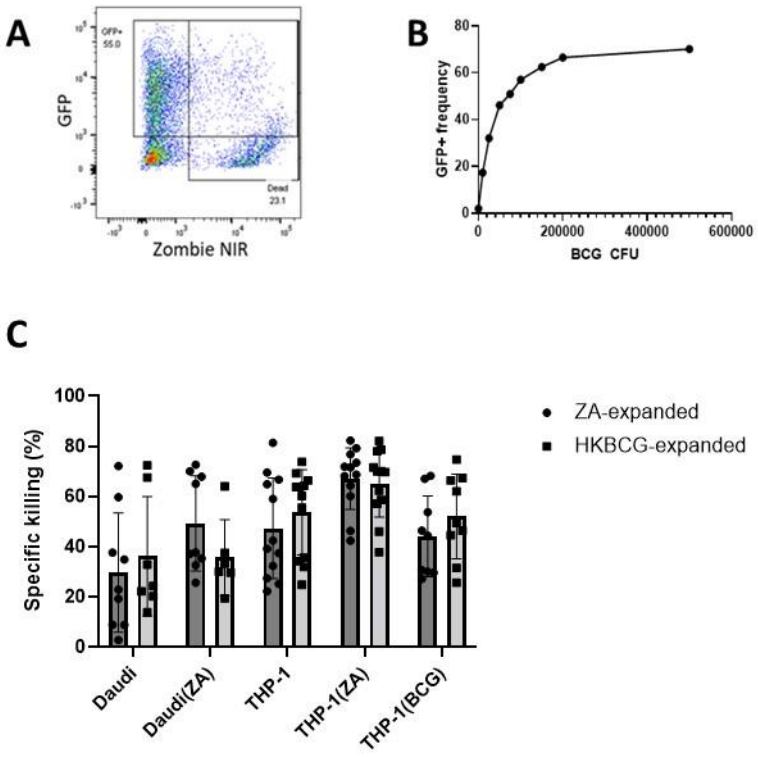

Figure 4

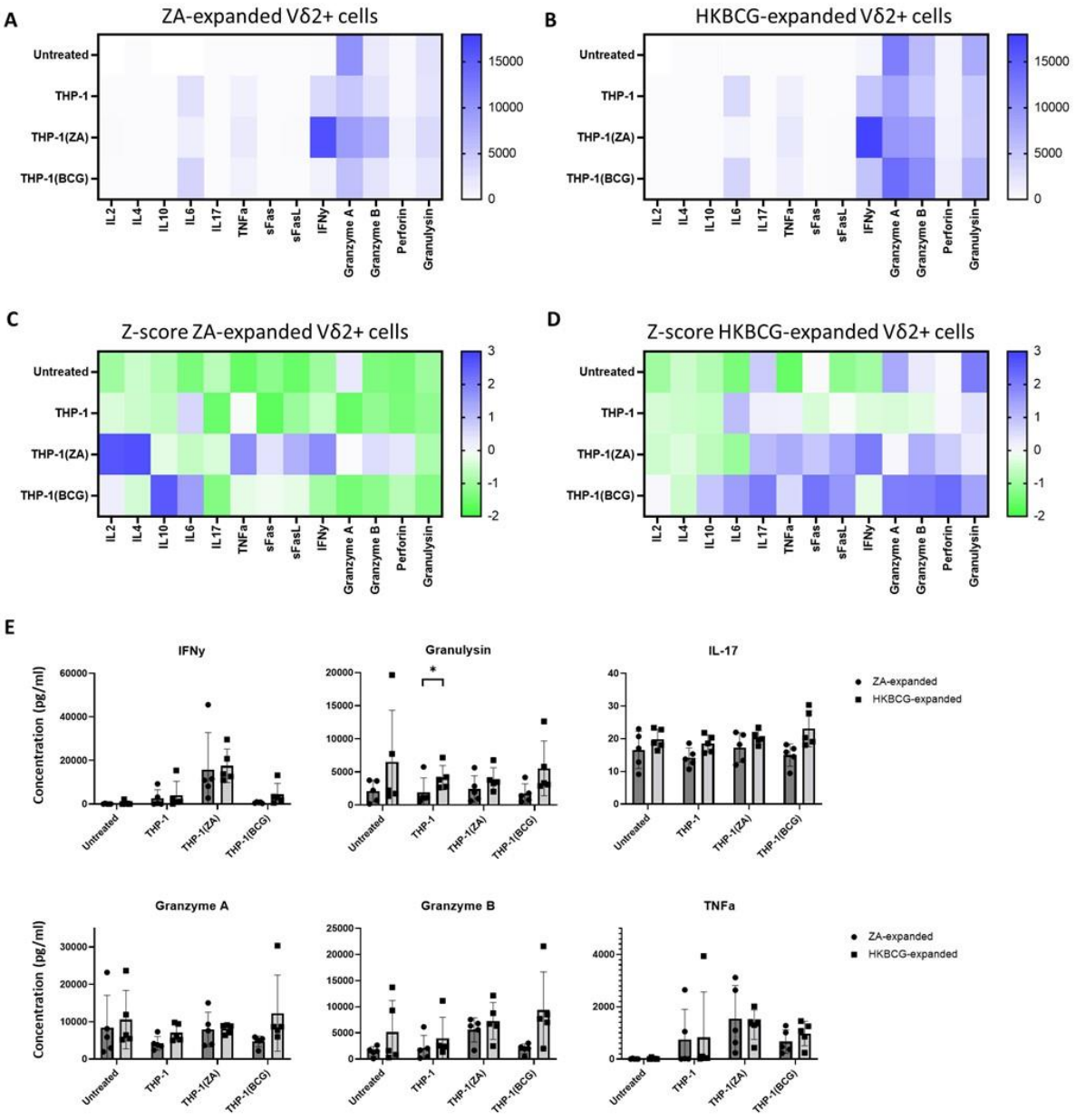

Figure 5

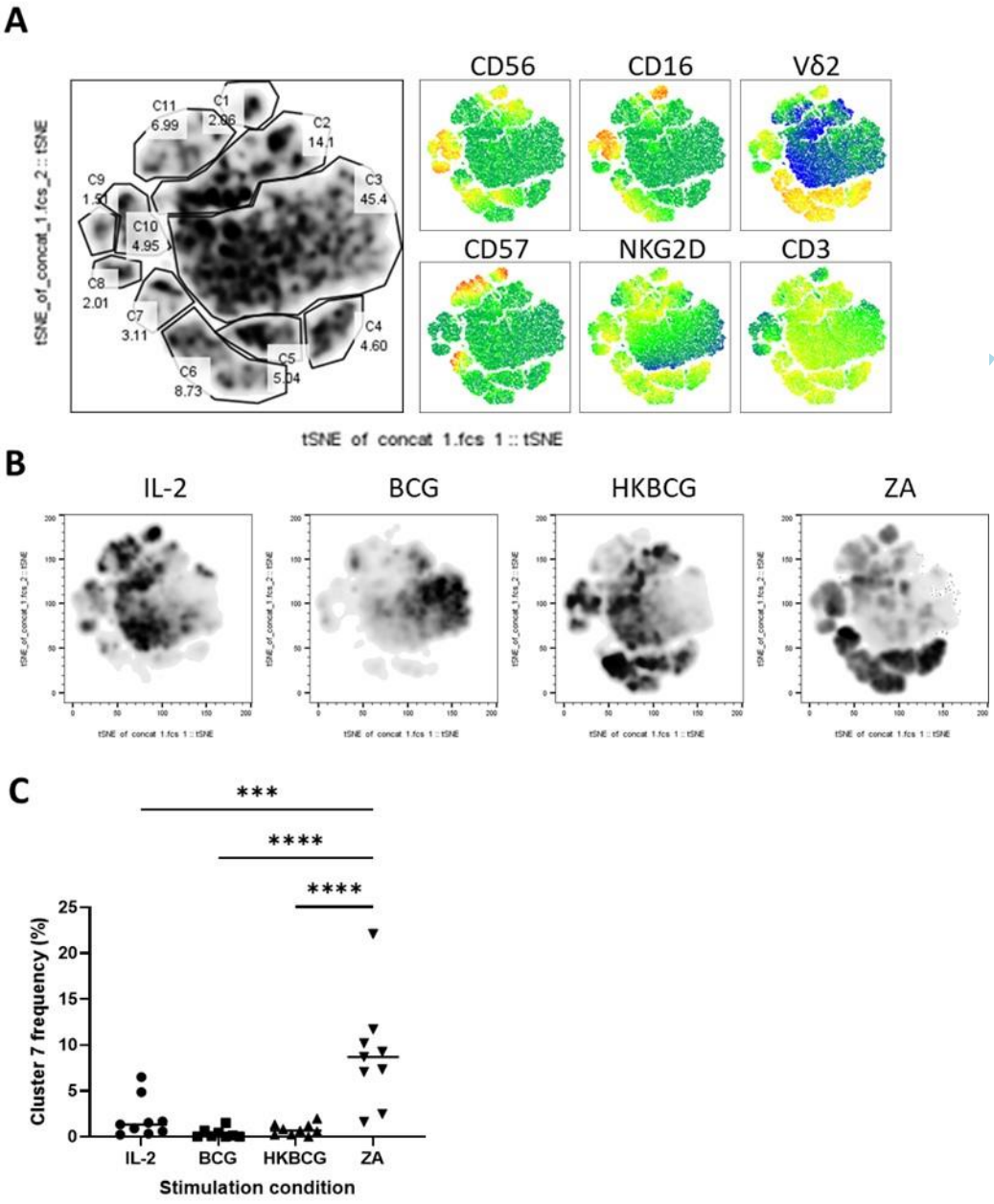

Figure 6

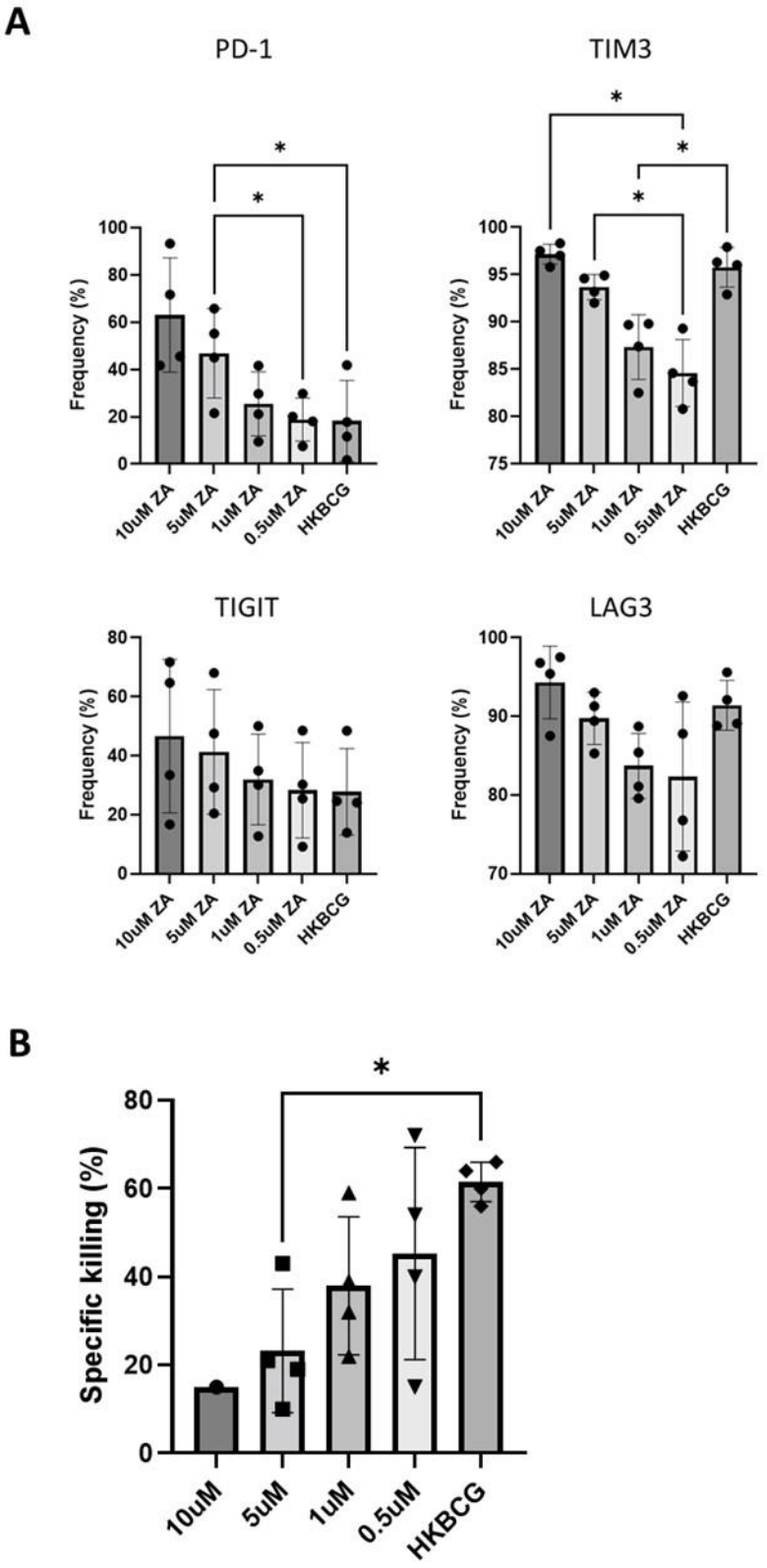

Figure 7